

Journal of Materials Chemistry A

Accepted Manuscript



This is an *Accepted Manuscript*, which has been through the Royal Society of Chemistry peer review process and has been accepted for publication.

Accepted Manuscripts are published online shortly after acceptance, before technical editing, formatting and proof reading. Using this free service, authors can make their results available to the community, in citable form, before we publish the edited article. We will replace this *Accepted Manuscript* with the edited and formatted *Advance Article* as soon as it is available.

You can find more information about *Accepted Manuscripts* in the [Information for Authors](#).

Please note that technical editing may introduce minor changes to the text and/or graphics, which may alter content. The journal's standard [Terms & Conditions](#) and the [Ethical guidelines](#) still apply. In no event shall the Royal Society of Chemistry be held responsible for any errors or omissions in this *Accepted Manuscript* or any consequences arising from the use of any information it contains.

ARTICLE

An In^{III}-based Anionic Metal–Organic Framework: Sensitization of Lanthanide (III) Ions and Selective Absorption and Separation of Cationic Dyes

Cite this: DOI:
10.1039/x0xx00000x

Received 00th January 2012,
Accepted 00th January 2012

DOI: 10.1039/x0xx00000x

www.rsc.org/

Lin Liu,^a Xiao-Nan Zhang,^a Zheng-Bo Han,^{a*} Ming-Liang Gao,^a Xiao-Man Cao,^a and Shi-Ming Wang^{b*}

Abstract: An In^{III}-based anionic framework (In^{III}-MOF) with 4-connected SrAl₂ topology was constructed. The In^{III}-MOF with permanent porosity functions as a host for encapsulation of Ln³⁺ ions through ion-exchange processes. The photophysical properties of as-prepared Ln³⁺@In^{III}-MOF were investigated and the results showed that the In^{III}-MOF could serve as an antenna to sensitize Ln³⁺ cations, especially suitable for Tb³⁺ and Eu³⁺ ions. The possible sensitization mechanism has been studied by surface photovoltage spectroscopy. Additionally, In^{III}-MOF could also as host materials applied in the separation and purification of cationic dyes, which is highly based on the size and charge of organic dyes. Moreover, it can be used as chromatographic column stationary phases to separate cationic dyes more efficiently and selectively. It is believed that the as-prepared In^{III}-MOF may provide potential applications in optical materials and environmental fields.

Introduction

Metal–Organic Frameworks (MOFs) have been widely investigated as functional materials in supramolecular chemistry, such as gas storage, ion-exchange, separation and fluorescent sensor.^[1] In particular, MOFs could provide a potential platform whose functions can be tuned through rational postsynthetic modification.^[2] Particularly, charged MOFs make the postsynthetic modification facile and controllable.^[3]

Lanthanide-based luminescent materials usually generate sharp fluorescent emissions with different colors. Therefore, engineering lanthanide-based MOFs is a sensible choice to gain the tunable luminescent materials.^[4] One way is using lanthanide ions as metal nodes of the MOFs^[5] and the different colors light emission could be achieved by altering the lanthanide ions of the isomorphous frameworks.^[6] Another way is encapsulating the lanthanide ions into a stable MOFs through postsynthetic process, which access the tunable luminescent materials by means of controlling the different type of guest species.^[7] Very recently, anionic MOFs provide an efficient media to capture and sensitize lanthanide cations to achieve luminescence materials with different colors.^[8] Notably, primary color light emissions were obtained by this simple method. When mix the two (blue and yellow) or three (blue, green, and red) primary colors together would generate white light emission.^[9] It is judicious to choose lanthanide cations as the guest of the anionic frameworks to obtain primary color emission. Petoud and co-workers reported porous anionic bio-MOF-1 which can incorporate lanthanide cations via cation-exchange process and sensitize multiple lanthanide cations, thus allowing for the facile preparation of multiple different luminescent materials.^[8a] Such progress in this field permits us to rationally design and synthesize ionic MOFs for specific host–guest materials.

In addition, the charged MOFs can be applied in absorption and separation of metal cations, as well as show great potential in the efficient separation of organic dyes.^[3c, 10] Especially, charged MOFs based ion-exchange chromatograph and ion-exchange solid phase extraction would be the powerful tools for the charged molecules separation.^[11] However, only a few examples of charged MOFs reported can be applied as ion-exchange chromatograph for dyes.^[12] Bu and co-workers reported positive frameworks, which could be selective separation for anionic dye molecules.^[12a] The selective separation of dyes are based on the following reasons: first, the counter ions could only be substituted by the same charged dye molecules; second, the pore size would determine what size of dyes could be as the guests of the framework. Therefore, the reasonable selection of the ligand and metal node would result in the charged framework and selective separation of dyes.

Up to now, there are a number of reports of In^{III}-based ionic frameworks. Most of the In^{III}-based frameworks are highly stable and show advanced functions.^[10d, 13] Exploring new In^{III}-based anionic frameworks is desirable. In this paper, an anionic framework with the formula of [(CH₃)₂NH₂][In(L)]·CH₃CH₂OH (In^{III}-MOF) (H₄L = 2,3',5,5'-biphenyl tetracarboxylic acid) was prepared utilizing solvothermal method. In^{III}-MOF could undergo ion-exchange process to encapsulate the lanthanide cations and separate cationic dyes. The In^{III}-MOF could serve as an antenna to sensitize Ln³⁺ cations, especially suitable for Tb³⁺ and Eu³⁺ ions. The mechanism of MOF sensitizing Ln³⁺ luminescence was first investigated by surface photovoltage spectroscopy technology in this work. Additionally, In^{III}-MOF presents excellent reversible absorption of cationic dyes and can serve as chromatographic column stationary phases to separate cationic dye molecules efficiently and selectively.

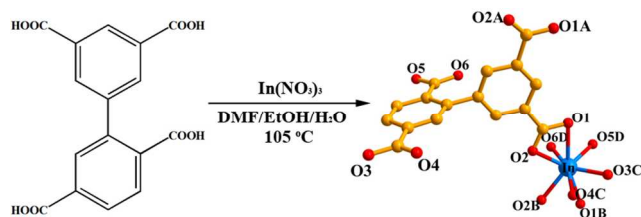
Experimental section

Materials and methods:

All starting materials and solvents employed were commercially available and used without further purification. X-ray powder diffraction was recorded with a Bruker AXS D8 advanced automated diffractometer with Cu-K α radiation. Thermogravimetric analyses (TGA) were taken on a Perkin-Elmer Pyris1 (25–700 °C, 5 °C min⁻¹, flowing N₂ (g)). Ar adsorption–desorption experiments were carried out on automated gas sorption analyzer (Quantachrome Instrument ASiQ-C). The C, H, and N microanalyses were carried out with Perkin-Elmer 240 elemental analyzer. Inductively Coupled Plasma-Optical Emission Spectroscopy (ICP) was measured by 700 Series ICP-OES (Agilent Technologies). The FT-IR spectra were recorded from KBr pellets in the range 4000–400 cm⁻¹ on a Nicolet 5DX spectrometer. Luminescence spectra and lifetimes of the solid samples were investigated with an FLSP920 Edinburgh Fluorescence Spectrometer at room temperature. The surface photovoltage spectroscopy measurement was recorded on a lab-made instrument, which constitutes a source of monochromatic light, a lock-in amplifier (SR830-DSP) with a light chopper (SR540) and a photovoltaic cell. A 500 W xenon lamp (CHF5000 W, Global xenon lamp power) and a double-prism monochromator (Hilger and Watts, D300) provide monochromatic light. The construction of the photovoltaic cell was a sandwich-like structure of ITO-sample-ITO. All UV/Vis spectra were measured on a SP-752(PC) UV-Vis spectrophotometer (Shanghai Spectrum Instrument Co., Ltd).

Preparation of [(CH₃)₂NH₂][In(L)]·CH₃CH₂OH (In^{III}-MOF):

A mixture of In(NO₃)₃ (15 mg, 0.16 mmol), H₄L (5 mg, 0.15 mmol), DMF/CH₃CH₂OH/H₂O (2:1:1, 2 mL) and one drops of 16 M HNO₃ was stirred in a glass vial for *ca.* 20 min at room temperature, which was heated in an oven to 378 K for 3 days, followed by slow cooling (5 K h⁻¹) to room temperature (Scheme 1). The colorless stick-like crystals In^{III}-MOF were obtained and washed with DMF and dried in air (yield: *ca.* 53%). The counter cation (CH₃)₂NH₂⁺ is generated via decomposition of the DMF solvent. Elemental analysis calcd (%) for In^{III}-MOF, C₂₀H₂₀InNO₉ (%): C 45.05, H 3.78, N 2.63; Found: C 45.56, H 3.56, N 2.43; IR (KBr pellets, cm⁻¹): 3451 (s), 2915 (w) 1665 (vs), 1587 (s), 1385 (vs), 1266 (m), 1096 (m), 862(m), 759 (m), 664 (w), 554 (m). The composition of In^{III}-MOF was confirmed by single crystal X-ray diffraction, elemental analysis and IR spectroscopy, in addition, the phase purity of the bulk sample was confirmed by powder X-ray diffraction (PXRD).



Scheme 1 Schematic representation of the synthesis of In^{III}-MOF. Symmetry codes: A: x, 1.5–y, z; B: 0.5–x, 1–y, 0.5+z; C: 0.5–x, 1–y, 0.5+z; D: 1–x, 1–y, 1–z.

X-ray Crystallography

Crystallographic data of the complex was collected at 293 K with a Apex CCD II diffractometer with Mo-K α radiation (λ = 0.71073 Å) and graphite monochromator using the ω -scan mode. The structure was solved by direct method and refined on F^2 by full-matrix least squares using the SHELXTL-97 crystallographic software package.^[14] (CH₃)₂NH₂⁺ cations and guest solution molecules were

highly disordered, and attempts to locate and refine the peaks were unsuccessful. The diffused electron densities resulting from these residual molecules were removed from the data set using the SQUEEZE^[15] routine of PLATON and refined further using the data generated. The contents of (CH₃)₂NH₂⁺ and guest molecules are not represented in the unit cell contents for the crystal data. Crystallographic data for structural analyses are summarized in Table S1. The CCDC reference number 1045476 for In^{III}-MOF. Copy of the data can be obtained free of charge on application to CCDC, 12 Union Road, Cambridge CB2 1EZ, UK [Fax: int code +44(1223)336-033; E-mail: deposit@ccdc.cam.ac.uk].

Encapsulation of Ln³⁺ cations in In^{III}-MOF

Ln(NO₃)₃ [Sm(NO₃)₃·6H₂O, Eu(NO₃)₃·6H₂O, Tb(NO₃)₃·5H₂O, and Dy(NO₃)₃·5H₂O] were used as purchased. A solution of Ln(NO₃)₃ in DMF (0.1 M) was prepared. Encapsulation of Ln³⁺ cations was performed as follows: the as-synthesized In^{III}-MOF was soaked in the Ln(NO₃)₃ solution and every 24 h changed with fresh solution for 3 days. After cation exchange was completed, the materials were thoroughly washed with DMF and soaked in DMF at least 24 h.

Experimental details for Organic dye selective adsorption and separation

Freshly prepared In^{III}-MOF (20 mg) was immersed in 5 mL DMF solutions of different organic dyes with the concentrations of 5 × 10⁻⁵ M. The release experiment was carried out after the completion of an ion-exchange process of Methylene blue (MB) on In^{III}-MOF. Then, the as prepared MB⁺@In^{III}-MOF was immersed in the saturated solution of NaCl in DMF with the same volume. Chromatographic column is made of bottomless NMR sample tube (Ø5 mm, 180 mm) and In^{III}-MOF was filled in the NMR sample tube (80 mm) as stationary phase. The DMF solutions of MB⁺, mixed MB⁺/MO⁻ (1:1), MB⁺/SD⁰ (1:1), and MB⁺/CV⁺ (1:1) (10⁻⁴ M, 3 mL) were used for separation.

Results and discussion

Crystal structure of In^{III}-MOF

The Single-crystal X-ray analysis reveals that In^{III}-MOF features a three-dimensional framework constructed from mononuclear [In(O₂CR)₄] nodes bridged by the tetracarboxylate ligand (L) (Fig. 1a). The counterions of (CH₃)₂NH₂⁺ are located in the channels to balance the charge. In the anionic framework, the four carboxylate groups of L ligand adopt chelating coordination mode to link four In^{III} ions. The In^{III} ion is eight-coordinate and surrounded by eight oxygen atoms from four individual L ligands. There are two different kinds of channels along the *b*-axis: the smaller quadrilateral channels of 5.22 × 6.85 Å² and larger quadrilateral channels of 9.17 × 14.43 Å² (measured between opposite atoms) in size (Fig. S1). The total accessible volume of In^{III}-MOF after the removal of the counter cations and guest solvent molecules is *ca.* 65.5% using PLATON.^[16] However, this void contains the disordered (CH₃)₂NH₂⁺ cations and guest solvent molecules. The (CH₃)₂NH₂⁺ cations are difficult to remove after the thermal activation, which give rise to the Ar uptake is relatively small (Fig. S2). Therefore, a Li⁺-exchanged sample In^{III}-MOF-Li⁺ was prepared by immersing crystals of In^{III}-MOF in a saturated solution of LiCl in DMF. As shown in Fig. S6, both Ar isotherms of In^{III}-MOF and In^{III}-MOF-Li⁺ exhibit typical Type-I adsorption behaviour confirming the retention of the microporous structures of the crystalline samples. The BET surface areas for In^{III}-MOF and In^{III}-MOF-Li⁺ were estimated as 182.8 and 554.1 m² g⁻¹, respectively, indicating that the adsorption capacity of In^{III}-MOF-Li⁺

increases significantly. From the topological point of view, if the L ligands and In^{III} ions are considered as 4-connected nodes, the 3D structure of In^{III} -MOF can be simplified as a uninodal four-connected SRA topology with Schläfli symbol of $4^2\cdot6^3\cdot8$, which is related to the structural prototype of SrAl_2 (or zeolite ABW)^[17] (Fig. 1b).

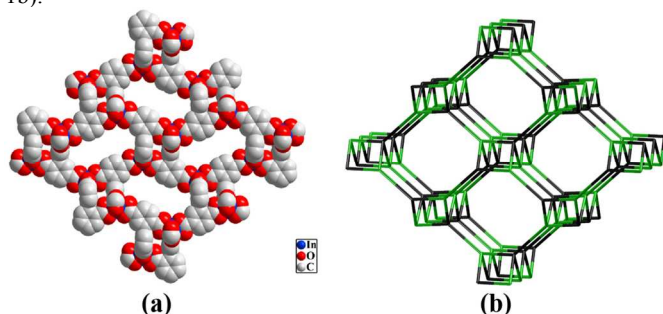


Fig. 1 (a) Space-filling representation of In^{III} -MOF along the b -axis; (b) View of the 3D four-connected framework of In^{III} -MOF can be represented as a four-connected net of SRA topology (the green nodes represent the In nodes, the black nodes represent the L_4 ligands).

Thermal Stability

The TGA curve of In^{III} -MOF displayed that the weight loss of the guest solvent molecules was well resolved (Fig. S3). The curve exhibits two major losses in the temperature range of 25–500 °C, the weight loss of 17.3 % during the first step between 25 and 250 °C corresponds to the loss of one guest $\text{CH}_3\text{CH}_2\text{OH}$ molecule and one free $(\text{CH}_3)_2\text{NH}_2^+$ cation (calculated 17.3 %). Decomposition of In^{III} -MOF began above 330 °C. The powder X-ray diffraction (PXRD) pattern for In^{III} -MOF shows that the diffraction peaks of both simulated and experimental patterns match well in key positions, indicating the phase purities of In^{III} -MOF (Fig. S4). Additionally, the In^{III} -MOF shows favorable water stability (Fig. S5), which is crucial for the development of its porous system in relevant applications.

Luminescence properties

Because of the anionic framework of In^{III} -MOF and $(\text{CH}_3)_2\text{NH}_2^+$ in the 1D channels, it makes the In^{III} -MOF suitable for exchanging of lanthanide cations to the host framework to form novel Ln -doped luminescent materials and new Ln^{3+} sensors through the antenna effect.^[4a] We tried to introduce lanthanide cations into the pores of In^{III} -MOF and then analyze the luminescent properties of the resulting $\text{Ln}^{3+}@\text{In}^{\text{III}}$ -MOF. ICP data of the Ln^{3+} exchanged materials revealed the doped amounts of the Ln^{3+} ions (Table S2). The molar ratio of $\text{In}^{3+}/\text{Ln}^{3+}$ was about 3:1, which suggested that one Ln^{3+} ion exchanged out approximately three $(\text{CH}_3)_2\text{NH}_2^+$ cations. The PXRD patterns (Fig. S6) and IR spectra (Fig. S7) of the $\text{Ln}^{3+}@\text{In}^{\text{III}}$ -MOF confirmed that the structure of In^{III} -MOF was maintained its crystalline integrity after the ion-exchange experiments. As expected, In^{III} -MOF succeeds to sensitize Tb^{3+} , Sm^{3+} , Eu^{3+} , and Dy^{3+} , which are confirmed from the emission spectra of the $\text{Ln}^{3+}@\text{In}^{\text{III}}$ -MOF. The excitation and emission spectra of the powder samples of H_4L are displayed in Fig. S8. The emission spectrum of In^{III} -MOF is shown in Fig. 2a. The H_4L ligand exhibits a strong emission at 420 nm with the excitation at 363 nm due to $\pi\text{-}\pi^*$ transitions. In^{III} -MOF exhibits more enhanced blue light emission and shift slightly to 447 nm with the excitation at 340 nm. Under the excitation at 340 nm, the $\text{Ln}^{3+}@\text{In}^{\text{III}}$ -MOF ($\text{Ln}^{3+} = \text{Tb}^{3+}$, Eu^{3+} , Sm^{3+} and Dy^{3+}) samples show a similar emission in the region 400–500 nm with different intensity. The emission spectrum of $\text{Tb}^{3+}@\text{In}^{\text{III}}$ -MOF emits its distinctive green color with typical Tb^{3+} ion emissions at $\lambda_{\text{em}} = 489$, 544, 583 and 622 nm (Fig. 2b), which correspond to the

characteristic transitions of $^5\text{D}_4 \rightarrow ^7\text{F}_j$ ($J = 3\text{--}6$) transitions. Two intense emission bands at $\lambda_{\text{em}} = 489$ and 544 due to the $^5\text{D}_4 \rightarrow ^7\text{F}_6$

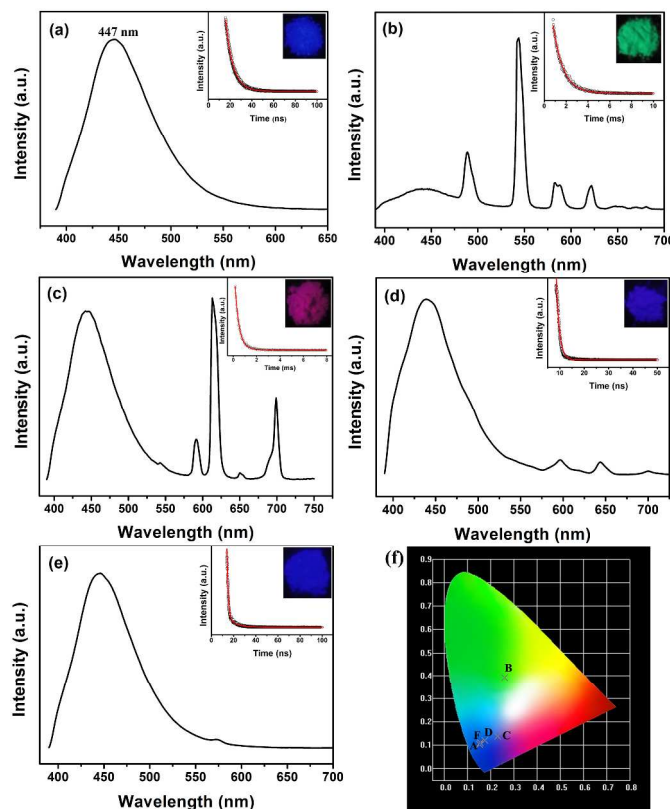
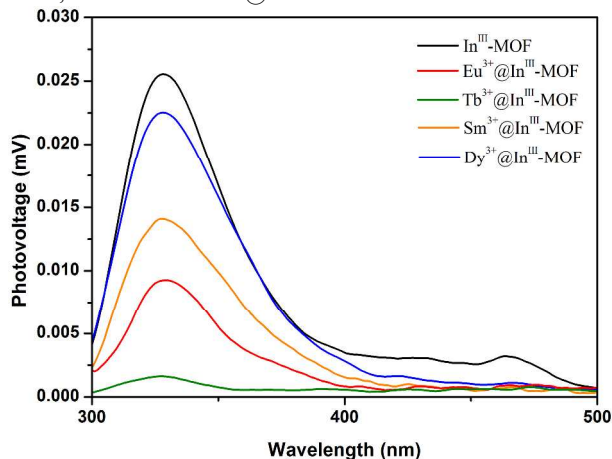


Fig. 2 Emission spectra of (a) In^{III} -MOF, (b) $\text{Tb}^{3+}@\text{In}^{\text{III}}$ -MOF, (c) $\text{Eu}^{3+}@\text{In}^{\text{III}}$ -MOF, (d) $\text{Sm}^{3+}@\text{In}^{\text{III}}$ -MOF and (e) $\text{Dy}^{3+}@\text{In}^{\text{III}}$ -MOF excited at 340 nm in the solid state at room temperature. Insets: Luminescence decay curves of (a) In^{III} -MOF, (b) $\text{Tb}^{3+}@\text{In}^{\text{III}}$ -MOF, (c) $\text{Eu}^{3+}@\text{In}^{\text{III}}$ -MOF, (d) $\text{Sm}^{3+}@\text{In}^{\text{III}}$ -MOF and (e) $\text{Dy}^{3+}@\text{In}^{\text{III}}$ -MOF; Photographs of the respective samples under a UV lamp; (f) CIE chromaticity diagram for In^{III} -MOF (A) and $\text{Ln}^{3+}@\text{In}^{\text{III}}$ -MOF (Tb^{3+} for B, Eu^{3+} for C, Sm^{3+} for D, and Dy^{3+} for E)

and $^5\text{D}_4 \rightarrow ^7\text{F}_5$ transitions, the weaker emission bands at $\lambda_{\text{em}} = 583$ and 622 nm originate from the $^5\text{D}_4 \rightarrow ^7\text{F}_4$ and $^5\text{D}_4 \rightarrow ^7\text{F}_3$ transitions. This phenomenon is associated with the emission intensity of In^{III} -MOF at ~447 nm decreases, and it is less pronounced as compared with the Tb^{3+} ion emissions. This result confirmed that the energy transfer from In^{III} -MOF to the Tb^{3+} centers efficiently. The spectrum is dominated by the $^5\text{D}_4 \rightarrow ^7\text{F}_5$ intense band and it is responsible for the brilliant green emission of the $\text{Tb}^{3+}@\text{In}^{\text{III}}$ -MOF hybrid. On the other hand, the emission spectrum of $\text{Eu}^{3+}@\text{In}^{\text{III}}$ -MOF emits its unique red color with characteristic emissions of the Eu^{3+} ion. As shown in Fig. 2c, the emission spectrum at $\lambda_{\text{em}} = 591$, 613, 650, and 699 nm are according to the typical Eu^{3+} ion emission which can be originated from the characteristic emission $^5\text{D}_0 \rightarrow ^7\text{F}_j$ ($J=1\text{--}4$) transitions. At the same time, the characteristic emission of In^{III} -MOF at $\lambda_{\text{em}} = 447$ still existed. The intense emission bands at $\lambda_{\text{em}} = 613$ nm due to the $^5\text{D}_0 \rightarrow ^7\text{F}_2$ transition. These results suggest that only part of energy transfer from In^{III} -MOF to the Eu^{3+} centers. Whereas, $\text{Sm}^{3+}@\text{In}^{\text{III}}$ -MOF shows two weak characteristic emissions at $\lambda_{\text{em}} = 596$ and 644 nm (Fig. 2d), which are typical Sm^{3+} ion emissions and correspond to the characteristic transitions of $^4\text{G}_{5/2} \rightarrow ^6\text{H}_j$ ($J=7/2, 9/2$) transitions. Similar to the situation, the emission spectrum of $\text{Dy}^{3+}@\text{In}^{\text{III}}$ -MOF emits a weak typical Dy^{3+} ion emission at $\lambda_{\text{em}} = 572$ nm (Fig. 2e), which can be attributed to the

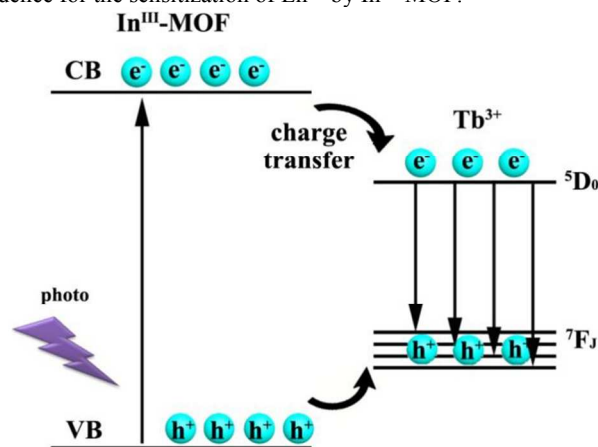
characteristic emission $^4F_{9/2} \rightarrow ^6H_{13/2}$. These results indicate that In^{III} -MOF acts as not only a host to encapsulation Ln^{3+} cations, but also serves as an antenna to sensitizes Ln^{3+} cations, especially suitable for Tb^{3+} and Eu^{3+} . Thus, the emission color modulated by the postsynthetic process of encapsulating different Ln^{3+} ions, which may gain white light emission. The corresponding CIE chromaticity coordinates diagram is shown in Fig. 2f. It is noteworthy that $\text{Tb}^{3+}@\text{In}^{\text{III}}$ -MOF and $\text{Eu}^{3+}@\text{In}^{\text{III}}$ -MOF show very long Ln^{3+} lifetimes. For example, $\tau = 919.63 \mu\text{s}$ for $\text{Tb}^{3+}@\text{In}^{\text{III}}$ -MOF; $\tau = 362.55 \mu\text{s}$ for $\text{Eu}^{3+}@\text{In}^{\text{III}}$ -MOF. However, the lifetimes of In^{III} -MOF, $\text{Sm}^{3+}@\text{In}^{\text{III}}$ -MOF and $\text{Dy}^{3+}@\text{In}^{\text{III}}$ -MOF are relatively short ($\tau = 6.83733 \text{ ns}$ for In^{III} -MOF; $\tau = 1.30488 \text{ ns}$ for $\text{Sm}^{3+}@\text{In}^{\text{III}}$ -MOF; $\tau_1 = 1.17343 \text{ ns}$ and $\tau_2 = 7.46201 \text{ ns}$ for $\text{Dy}^{3+}@\text{In}^{\text{III}}$ -MOF). When illuminated with a standard laboratory UV lamp ($\lambda_{\text{ex}} = 254 \text{ nm}$), the doped materials displayed strong luminescence which can be easily observed by the naked eye.

The surface photovoltage spectroscopy (SPS) technique was used for investigating the photophysics of the excited states and the surface charge behavior of the materials. It is an efficient method to reveal the fundamental feature of separation and transport of photogenerated charges.^[18] The possible sensitization mechanism for the above phenomenon is proposed as follows. As shown in Fig. 3, the SPS spectra are the as-prepared In^{III} -MOF and $\text{Ln}^{3+}@\text{In}^{\text{III}}$ -MOF samples. In^{III} -MOF presents positive SPV response band in the region of 300–400 nm and the photovoltage response centered at 329 nm. It indicates that In^{III} -MOF possesses semiconductor characteristic. When the light illuminated the surface of In^{III} -MOF, the electrons (e^-) in the valence band (VB) were excited to the conduction band (CB), and holes (h^+) were left in the VB. Driven by the built-in field, the electrons and holes move to the opposite directions, which results in different expression of the surface potential and generating a photovoltage signal. With the encapsulation of Ln^{3+} ions, the intensities of the SPS response decrease obviously. The weakened SPS response demonstrates that only a small part of the photogenerated charges are separated, while most other photogenerated charges are involved in the sensitization process in $\text{Ln}^{3+}@\text{In}^{\text{III}}$ -MOF samples, which due to the intensity of SPS reflects the separation efficiency of photogenerated charges.^[19] As shown in Scheme 2, for the $\text{Tb}^{3+}@\text{In}^{\text{III}}$ -MOF, the energy level of conduction band of In^{III} -MOF is higher than that of the emitting state (5D_4) of Tb^{3+} ions. Thus, the photogenerated electrons can transfer to the $5d$ level of Tb^{3+} . At the same time, holes are inclined to transfer to $4f$ level, resulting in improved photoluminescent performance through a radiative transition process. That is to say, Tb^{3+} ions act as recombination centers to accelerate the recombination of process, which facilitate the electron transfer from In^{III} -MOF to Ln^{3+} . However, the different $\text{Ln}^{3+}@\text{In}^{\text{III}}$ -MOF results in the different SPS



response and the intensity of the SPS is consistent with the degree of

Ln^{3+} ions sensitized by In^{III} -MOF. That's might be attributed to the Fig. 3 SPS of In^{III} -MOF and $\text{Ln}^{3+}@\text{In}^{\text{III}}$ -MOF samples. different match degrees of the energy level between Ln^{3+} ions and In^{III} -MOF. In this connection, the SPS results provide a convincing evidence for the sensitization of Ln^{3+} by In^{III} -MOF.

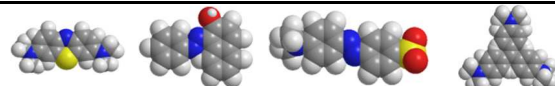


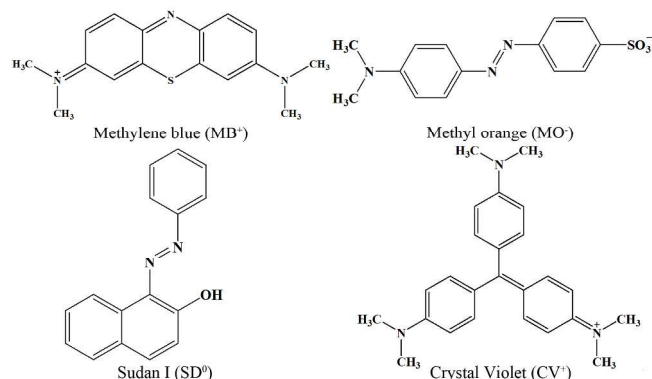
Scheme 2 Transfer and separation of photogenerated charges in $\text{Tb}^{3+}@\text{In}^{\text{III}}$ -MOF.

Organic dye selective adsorption and separation

Currently, dyes are widely used in many industries and the removal of dyes from waste water has been attracting intense attention from an environmental point of view.^[20] To investigate the capacity of In^{III} -MOF in separation dye molecules, we used In^{III} -MOF to capture dyes in DMF solutions. During the dye adsorption and separation process, charge and size of the organic dye are the two most important factors.^[12a] We have chosen four organic dyes for this study: Methylene blue (MB^+), Sudan I (SD^0), Methyl orange (MO^-) and Crystal Violet (CV^+) (Scheme 2). Firstly, we selected MB^+ , SD^0 and MO^- to investigate the absorption of organic dyes. These dyes features the similar size and molecular weight but different charges (Table 1). The fresh as-prepared In^{III} -MOF was immersed in the DMF solution of MB^+ , SD^0 and MO^- without disturbing. The content of dye in the solution was detected by certain time intervals using UV-vis absorption spectroscopy. As shown in Fig. 4a and Fig. 5, the Abs peak value of the solution was declined gradually up to 22 h, suggesting that nearly all the MB^+ was absorbed by the In^{III} -MOF. At the same time, the color of the solution fades to transparent. On the contrary, the colors of MO^- (Fig. S9) and SD^0 (Fig. S10) solutions detected no changes at all. What is more, in order to further demonstrate In^{III} -MOF adsorb MB^+ selectively, the mixtures of MB^+/SD^0 and MB^+/MO^- solutions were used. As shown in Fig. 4b and Fig. 4c, the results were as expected:

Table 1 Molecular weight and dimensions of different dyes molecules.

				
Abbr.	MB^+	SD^0	MO^-	CV^+
M_w	284.40	248.28	304.33	372.53
$x(\text{\AA})$	4.00	3.68	5.31	4.00
$y(\text{\AA})$	7.93	9.74	7.25	16.32
$z(\text{\AA})$	16.34	13.55	17.39	14.15



Scheme 2 Chemical structures of MB^+ , SD^0 , MO^- and CV^+ .

only the MB^+ was absorbed by the In^{III} -MOF in the mixture solutions and the solutions exhibited the colors of SD^0 and MO^- at last; and the color of In^{III} -MOF changed from colorless to blue. This phenomenon was attributed to the free $(\text{CH}_3)_2\text{NH}_2^+$ cations present in the channel of In^{III} -MOF. Therefore, In^{III} -MOF was only capable of adsorbing cationic dyes through ion-exchange and could not adsorb neutral and anionic dyes. The organic dyes with similar sizes but different charges could be selectively separated utilizing ion-exchange processes.

In order to study the size effect, two kinds of cationic dyes with different sizes were chosen: MB^+ and CV^+ . They have the same charges but different molecular sizes. CV^+ takes on a larger appearance (Table 1). Typically, the fresh crystalline samples of In^{III} -MOF were immersed into DMF solutions of MB^+ and CV^+ ; and the concentration changes were monitored by UV-vis absorbance at different time intervals. As shown in Fig. 4a and Fig. S11, for the smaller size MB^+ , the concentration of the solution declined sharply. However, for the large size CV^+ , it presents a totally different situation that the concentration of CV^+ in DMF almost no changed. The size selective effect was also tested under mixed solution of MB^+/CV^+ . As shown in Fig 4d, only characteristic peaks of MB^+ decreased significantly. Accordingly, only MB^+ was exchanged by

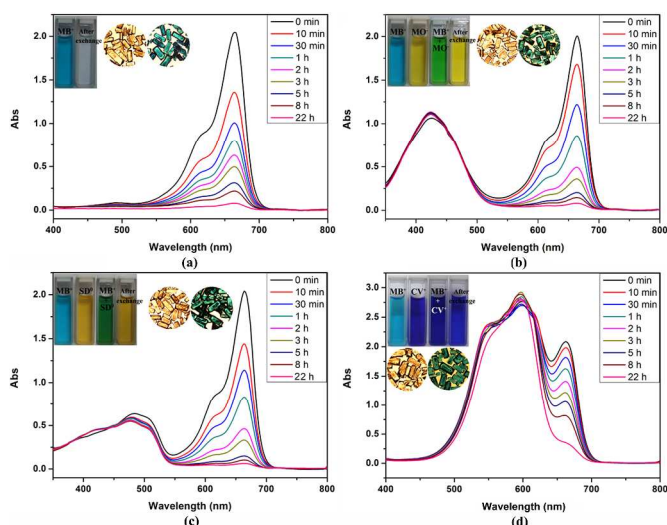


Fig. 4 UV-vis spectra of DMF solutions of equimolar dyes in the presence of In^{III} -MOF monitored with time: (a) MB^+ , (b) MB^+/MO^- , (c) MB^+/SD^0 , (d) MB^+/CV^+ . The photographs show the colors of the dye solutions and the crystalline samples of In^{III} -MOF, before and after ion-exchange for 22 h.

the In^{III} -MOF and crystal color also changed from colorless to blue, meanwhile the solution changed from blue-violet to purple. The molecular dimensions of MB^+ dye are 4.00 and 7.93 Å along the x and y directions, respectively, which are much smaller than the diameter of the channel for In^{III} -MOF (9.17×14.43 Å). Thus, MB^+ can enter into the channel of In^{III} -MOF smoothly. With respect to the CV^+ , the molecular dimensions along the x and y directions are 4.00 and 16.32, respectively, they are much larger than the diameter of the channel of In^{III} -MOF. As a result, CV^+ can't finish the ion-exchange process with In^{III} -MOF. Such observation again indicated that the ion-exchange process is size-dependent, which controlled by the size of the organic dye. If the dye is too large to diffuse into the channel of In^{III} -MOF, ion-exchange cannot be completed.

The reversibility and stability of the In^{III} -MOF after dye absorption and desorption is also an important criterion for real use. The dye release experiments are also carried out using the $\text{MB}^+@ \text{In}^{\text{III}}$ -MOF. Typically, $\text{MB}^+@ \text{In}^{\text{III}}$ -MOF was soaked in the saturated NaCl DMF solution and we used UV-vis spectrum detecting the concentration of dye in the solution. As shown in Fig. 5 and Fig. S12, the concentration of MB^+ in DMF solution increased gradually. Solution changed from colorless to blue color, with the color of the crystal turned back to colorless. This phenomenon is attributed to the ion exchange process, which is reversible and based on the dynamic equilibrium between different guests.^[12a] As a result, the Na^+ could enter into the channel of In^{III} -MOF instead of MB^+ when the concentration of Na^+ cation is large enough. The PXRD of In^{III} -MOF after release experiment confirmed the stability of the host crystal material (Fig. S13). It can be concluded the skeleton of the In^{III} -MOF did not change after the dye release. High efficiency selective absorption of dyes inspired us to use In^{III} -MOF as the stationary phase of an ion chromatographic column. The solution of MB^+ and mixed solutions of MB^+/MO^- , MB^+/SD^0 and MB^+/CV^+ with the same concentration were injected into the chromatographic column respectively. After the injection, we took the photos of the columns 3 minutes later. As shown in Fig. 6, MB^+ are quickly adsorbed onto the In^{III} -MOF and remained at the top of the chromatographic column (Fig. 6b), while MO^- (Fig. 6c), SD^0 (Fig. 6d) and CV^+ (Fig. 6e) were transported through the column, thus resulting in the separation. This phenomenon could be easily observed by the naked eye. From the above experiments, we can further deduce that In^{III} -MOF could serve as a good adsorbent to remove cationic dye molecules efficiently and selectively.

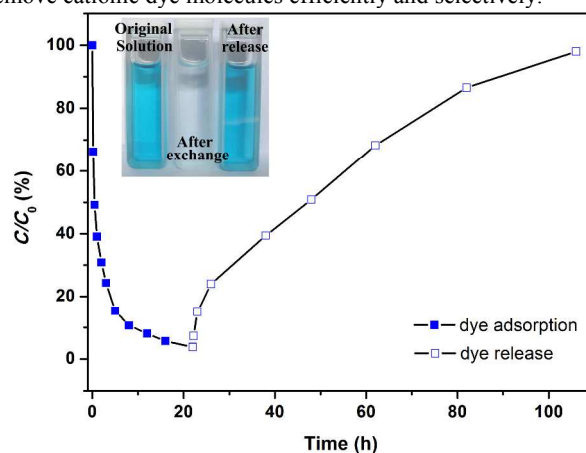


Fig. 5 The reversible absorbing and releasing of MB^+ in a full ion-exchange and release cycle.

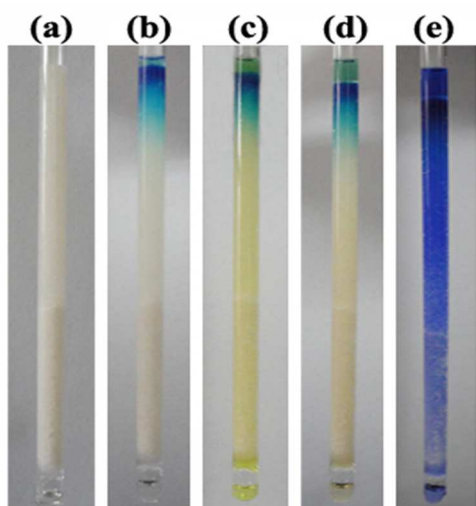


Fig. 6 Photograph for the as-prepared In^{III} -MOF -filled column-chromatographic (a); separation process for MB^+ (b), MB^+/MO^- (c), MB^+/SD^0 (d), and MB^+/CV^+ (e).

Conclusion

In summary, a new anionic In^{III} -based porous MOF with SrAl_2 topology has been synthesized and characterized, which exhibits an excellent host of encapsulation and sensitization for Ln^{3+} cations, especially suitable for Tb^{3+} and Eu^{3+} ions, and presents highly selective absorption and separation of cationic dyes *via* ion-exchange processes. The mechanism of In^{III} -MOF sensitizing Ln^{3+} luminescence was investigated by the SPS technology, which indicated that the Ln^{3+} ions act as electronic recombination centers and accelerate electron transfer from the In^{III} -MOF to Ln^{3+} . In addition, In^{III} -MOF can be used as ion chromatography stationary phases for the selective separation of cationic organic dyes, which could be applied in the environmental fields. Ongoing work is focused on applying ionic frameworks *via* ion-exchange process to fabricate functional materials with versatile properties like catalysis, adsorption, separation, luminescent materials and devices etc.

Acknowledgements

This work was granted financial support from National Natural Science Foundation of China (Grant 20871063, 21271096), the Liaoning Natural Science Foundation, China (20141052).

Notes and references

^a College of Chemistry, Liaoning University, Shenyang 110036 P. R. China E-mail: ceshzb@lnu.edu.cn (Z.-B. Han)

^b College of Light Industry, Liaoning University, Shenyang 110036 P. R. China E-mail: wangsm383@163.com (S.-M. Wang)

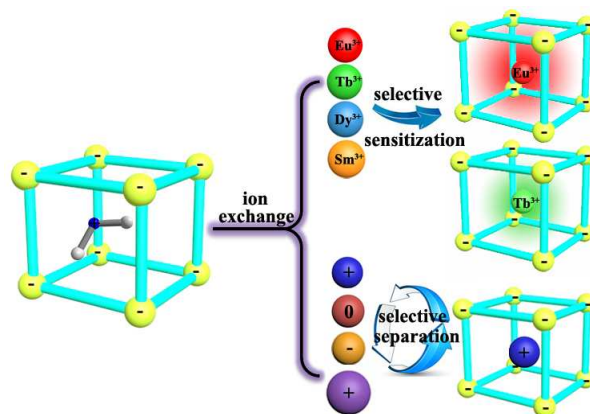
[†] Electronic Supplementary Information (ESI) available: the luminescence spectrum of the H_4L ligands, the TG curves of In^{III} -MOF, the PXRD patterns of In^{III} -MOF, and more informations about the crystal structures are available. See DOI: 10.1039/b000000x/

- (a) H. Furukawa, N. Ko, Y. B. Go, N. Aratani, S. B. Choi, E. Choi, A. O. Yazaydin, R. Q. Snurr, M. O'Keeffe, J. Kim, O. M. Yaghi, *Science*, 2010, **329**, 424–428; (b) M. Eddaoudi, D. F. Sava, J. F. Eubank, K. Adil, V. Guillermin, *Chem. Soc. Rev.*, 2015, **44**, 228–249; (c) D. Maspocho, D. Ruiz-Molina, K. Wurst, N. Domingo, M. Cavallini, F. Biscarini, J. Tejada, C. Rovira, J. Veciana, *Nat. Mater.*, 2003, **2**, 190–

- 195; (d) S. Stepanow, M. Lingenfelder, A. Dmitriev, H. Spillmann, E. Delvigne, N. Lin, X. Deng, C. Cai, J. V. Barth and K. Kern, *Nat. Mater.*, 2004, **3**, 229–233; (e) S. Horike, S. Shimomura, S. Kitagawa, *Nat. Chem.*, 2009, **1**, 695–704.
- (a) M. Banerjee, S. Das, M. Yoon, H. J. Choi, M. H. Hyun, S. M. Park, G. Seo, K. Kim, *J. Am. Chem. Soc.*, 2009, **131**, 7524–7525; (b) T. Gadzikwa, O. K. Farha, K. L. Mulfort, J. T. Hupp, S. T. Nguyen, *Chem. Commun.*, 2009, 3720–3722; (c) B. Li, Y. Zhang, D. Ma, L. Li, G. Li, Z. Shi, S. Feng, *Chem. Commun.*, 2012, **48**, 6151–6153; (d) V. Valtchev, G. Majano, S. Mintova, J. Perez-Ramirez, *Chem. Soc. Rev.*, 2013, **42**, 263–290; (e) M. H. Zeng, Z. Yin, Y. X. Tan, W. X. Zhang, Y. P. He, *J. Am. Chem. Soc.*, 2014, **136**, 4680–4688.
- (a) N. Ko, K. Noh, S. Sung, H. J. Park, S. Y. Park, J. Kim, *Chem. Commun.*, 2014, **50**, 6785–6788; (b) C. Mao, R. A. Kudla, F. Zuo, X. Zhao, L. J. Mueller, X. Bu, P. Feng, *J. Am. Chem. Soc.*, 2014, **136**, 7579–7582; (c) Y. X. Tan, Y. P. He, J. Zhang, *Chem. Commun.*, 2014, **50**, 6153–6156; (d) J. Yu, Y. Cui, C. Wu, Y. Yang, Z. Wang, M. O'Keeffe, B. Chen, G. Qian, *Angew. Chem. Int. Ed.*, 2012, **51**, 10542–10545; (e) J. Yu, Y. Cui, H. Xu, Y. Yang, Z. Wang, B. Chen, G. Qian, *Nat. Commun.*, 2013, **4**, 2719; (f) Z. Chen, Y. Sun, L. Zhang, D. Sun, F. Liu, Q. Meng, R. Wang and D. Sun, *Chem. Commun.*, 2013, **49**, 11557–11559.
- (a) M. D. Allendorf, C. A. Bauer, R. K. Bhakta, R. J. Houk, *Chem. Soc. Rev.*, 2009, **38**, 1330–1352; (b) Y. Jiao, J. Wang, P. Wu, L. Zhao, C. He, J. Zhang, C. Duan, *Chem.–Eur. J.*, 2014, **20**, 2224–2231; (c) H. Li, W. Shi, K. Zhao, Z. Niu, H. Li, P. Cheng, *Chem.–Eur. J.*, 2013, **19**, 3358–3365; (d) P. Wang, J. P. Ma, Y. B. Dong, and R. Q. Huang, *J. Am. Chem. Soc.*, 2007, **129**, 10620–10621; (e) G. He, D. Guo, C. He, X. Zhang, X. Zhao, and C. Duan, *Angew. Chem. Int. Ed.*, 2009, **48**, 6132–6135.
- (a) Y. Cui, B. Chen, G. Qian, *Coordin. Chem. Rev.*, 2014, **273–274**, 76–86; (b) L. E. Kreno, K. Leong, O. K. Farha, M. Allendorf, R. P. V. Duyne, J. T. Hupp, *Chem. Rev.*, 2012, **112**, 1105–1125; (c) Y. Li, S. Zhang, D. Song, *Angew. Chem. Int. Ed.*, 2013, **52**, 710–713; (d) Q. Tang, S. Liu, Y. Liu, J. Miao, S. Li, L. Zhang, Z. Shi, Z. Zheng, *Inorg. Chem.*, 2013, **52**, 2799–2801.
- (a) Z. Hu, B. J. Deibert, J. Li, *Chem. Soc. Rev.*, 2014, **43**, 5815–5840; (b) Y. Wang, J. Yang, Y. Y. Liu, J. F. Ma, *Chem.–Eur. J.*, 2013, **19**, 14591–14599; (c) K. A. White, D. A. Chengelis, K. A. Gogick, J. Stehman, N. L. Rosi, S. Petoud, *J. Am. Chem. Soc.*, 2009, **131**, 18069–18071.
- (a) J. Park, D. Feng, H. C. Zhou, *J. Am. Chem. Soc.*, 2015, DOI: 10.1021/ja5123528; (b) Y. Q. Lan, H. L. Jiang, S. L. Li, and Qiang Xu, *Adv. Mater.*, 2011, **23**, 5015–5020; (c) F. Luo, and S. R. Batten, *Dalton Trans.*, 2010, **39**, 4485–4488.
- (a) J. An, C. M. Shade, D. A. Chengelis-Czegán, S. Petoud, N. L. Rosi, *J. Am. Chem. Soc.*, 2011, **133**, 1220–1223; (b) J. S. Qin, S. R. Zhang, D. Y. Du, P. Shen, S. J. Bao, Y. Q. Lan, Z. M. Su, *Chem.–Eur. J.*, 2014, **20**, 5625–5630.
- (a) Y. P. He, Y. X. Tan, J. Zhang, *J. Mater. Chem. C* 2014, **2**, 4436–4441; (b) M. L. Ma, C. Ji, S. Q. Zang, *Dalton Trans.*, 2013, **42**, 10579–10586; (c) M. L. Ma, J.-H. Qin, C. Ji, H. Xu, R. Wang, B. J. Li, S. Q. Zang, H. W. Hou, S. R. Batten, *J. Mater. Chem. C*, 2014, **2**, 1085–1093.
- (a) H. Fei, D. L. Rogow, S. R. J. Oliver, *J. Am. Chem. Soc.*, 2010, **132**, 7202–7209; (b) Y.-C. He, J. Yang, W.-Q. Kan, H.-M. Zhang, Y.-Y. Liu, J.-F. Ma, *J. Mater. Chem. A*, 2014, **3**, 1675–1681; (c) Oliver, S. R. J. *Chem. Soc. Rev.*, 2009, **38**, 1868–1881; (d) S. Yang, X. Lin, A. J. Blake, K. M. Thomas, P. Hubberstey, N. R. Champness, M. Schröder, *Chem. Commun.*, 2008, 6108–6110.
- (a) R. Custelcean, B. A. Moyer, *Eur. J. Inorg. Chem.*, 2007, 1321–1340; (b) S. Yang, X. Lin, A. J. Blake, G. S. Walker, P. Hubberstey, N. R. Champness and M. Schröder, *Nat. Chem.*, 2009, **1**, 487–493.
- (a) X. Zhao, X. Bu, T. Wu, S. T. Zheng, L. Wang, P. Feng, *Nat. Commun.*, 2013, **4**, 2344; (b) Z. Zhu, Y. L. Bai, L. Zhang, D. Sun, J. Fang, and S. Zhu, *Chem. Commun.*, 2014, **50**, 14674–14677.
- (a) S. Yang, G. S. Martin, J. J. Titman, A. J. Blake, D. R. Allan, N. R. Champness, M. Schröder, *Inorg. Chem.*, 2011, **50**, 9374–9384; (b) S. Yang, S. K. Callear, A. J. Ramirez-Cuesta, W. I. F. David, J. Sun, A. J. Blake, N. R. Champness, M. Schröder, *Faraday Discuss.*, 2011, **151**, 19–36; (c) Y. Liu, J. F. Eubank, A. J. Cairns, J. Eckert, V. Ch. Kravtsov, R. Luebke, and M. Eddaoudi, *Angew. Chem. Int. Ed.*, 2007, **46**, 3278–3283; (d) S. Huh, T.-H. Kwon, N. Park, S.-J. Kim, Y. Kim,

- Chem. Commun.*, 2009, 4953–4955; (e) S. Chen, J. Zhang, T. Wu, P. Feng, and X. Bu, *J. Am. Chem. Soc.*, 2009, **131**, 16027–16029; (f) S. Yang, X. Lin, A. J. Blake, G. S. Walker, P. Hubberstey, N. R. Champness and M. Schröder, *Nat. Chem.*, 2009, **1**, 487–493.
14. G. M. Sheldrick, SHELXL-97, Programs for X-ray Crystal Structure Solution, University of Göttingen, Göttingen, Germany, 1997.
15. (a) K. Koh, A. G. Wong-Foy and A. J. Matzger, *Angew. Chem. Int. Ed.*, 2008, **47**, 677–680; (b) S. Hu, K. H. He, M. H. Zeng, H. H. Zou and Y. M. Jiang, *Inorg. Chem.*, 2008, **47**, 5218–5224.
16. (a) A. L. Spek, *J. Appl. Crystallogr.*, 2003, **36**, 7–13; (b) P. v. d. Sluis and A. L. Spek, *Acta Crystallogr. Sect. A*, 1990, **46**, 194–201.
17. (a) M. Du, Z. H. Zhang, L. F. Tang, X. G. Wang, X. J. Zhao and S. R. Batten, *Chem.–Eur. J.*, 2007, **13**, 2578–2586; (b) V. A. Blatov, L. Carlucci, G. Ciani and D. M. Proserpio, *CrystEngComm*, 2004, **6**, 377–395.
18. (a) S. Z. Li, J. W. Zhao, P. T. Ma, J. Du, J. Y. Niu, J. P. Wang, *Inorg. Chem.*, 2009, **48**, 9819–9830. (b) L. P. Sun, S. Y. Niu, J. Jin, L. Zhang, *Eur. J. Inorg. Chem.*, 2007, 3845–3852.
19. (a) X. Wei, T. F. Xie, Y. Zhang, D. J. Wang, J. S. Chen, *Mater. Chem. Phys.*, 2010, **122**, 259–261; (b) L. Jing, X. Sun, J. Shang, W. Cai, Z. Xu, Y. Du, H. Fu, *Sol. Energy Mater. Sol. Cells* 2003, **79**, 133–151.
20. (a) C. Y. Sun, X. L. Wang, C. Qin, J. L. Jin, Z. M. Su, P. Huang, K. Z. Shao, *Chem.–Eur. J.*, 2013, **19**, 3639–3645; (b) Z. Zhu, Y. L. Bai, L. Zhang, D. Sun, J. Fang, S. Zhu, *Chem. Commun.*, 2014, **50**, 14674–14677; (c) W. Zhang, J. Zhang, Z. Chen, T. Wang, *Catal. Commun.*, 2009, **10**, 1781–1785; (d) R. Zhang, S. Ji, N. Wang, L. Wang, G. Zhang, and J. R. Li, *Angew. Chem. Int. Ed.*, 2014, **53**, 9775–9779.

Table of Content



An In^{III}-based anionic MOF exhibits sensitization of Lanthanide (III) ions as well as absorption and separation of cationic dyes *via* ion-exchange.